



Assessing and optimizing the hydrological performance of Grey-Green infrastructure systems in response to climate change and non-stationary time series

Mo Wang ^{a,b}, Ming Liu ^a, Dongqing Zhang ^c, Jinda Qi ^{d,*}, Weicong Fu ^e, Yu Zhang ^a, Qiuyi Rao ^{a,b}, Amin E. Bakhshipour ^f, Soon Keat Tan ^g

^a College of Architecture and Urban Planning, Guangzhou University, Guangzhou 510006, China

^b Architectural Design and Research Institute of Guangzhou University, Guangzhou 510499, China

^c Guangdong Provincial Key Laboratory of Petrochemical Pollution Processes and Control, School of Environmental Science and Engineering, Guangdong University of Petrochemical Technology, Maoming, Guangdong 525000, China

^d Department of Architecture, National University of Singapore, 117575, Singapore

^e College of Landscape Architecture, Fujian Agriculture and Forestry University, Fuzhou 350002, China

^f Civil Engineering, Institute of Urban Water Management, University of Kaiserslautern, Kaiserslautern 67663, Germany

^g School of Civil and Environmental Engineering, Nanyang Technological University, 639798, Singapore

ARTICLE INFO

Keywords:

Urban stormwater management
Green infrastructure
Coupled Grey-Green system
Climate change
Regional climate model
Antecedent dry days

ABSTRACT

Climate change has led to the increased intensity and frequency of extreme meteorological events, threatening the drainage capacity in urban catchments and densely built-up cities. To alleviate urban flooding disasters, strategies coupled with green and grey infrastructure have been proposed to support urban stormwater management. However, most strategies rely largely on diachronic rainfall data and ignore long-term climate change impacts. This study described a novel framework to assess and to identify the optimal solution in response to uncertainties following climate change. The assessment framework consists of three components: (1) assess and process climate data to generate long-term time series of meteorological parameters under different climate conditions; (2) optimise the design of Grey-Green infrastructure systems to establish the optimal design solutions; and (3) perform a multi-criteria assessment of economic and hydrological performance to support decision-making. A case study in Guangzhou, China was carried out to demonstrate the usability and application processes of the framework. The results of the case study illustrated that the optimised Grey-Green infrastructure could save life cycle costs and reduce total outflow (56–66%), peak flow (22–85%), and TSS (more than 60%) compared to the fully centralised grey infrastructure system, indicating its high superior in economic competitiveness and hydrological performance under climate uncertainties. In terms of spatial configuration, the contribution of green infrastructure appeared not as critical as the adoption of decentralisation of the drainage networks. Furthermore, under extreme drought scenarios, the decentralised infrastructure system exhibited an exceptionally high degree of removal performance for non-point source pollutants.

1. Introduction

Rapid urbanisation leads to a significant increase of impermeable surfaces, resulting in increased surface runoff and thereby threatening

the hydrological safety of cities and waterlog ([Larsen et al., 2016](#); [Nazari-Sharabian et al., 2019](#)). [Aerts et al. \(2014\)](#) reported that urban waterlog caused direct economic losses of \$650 billion over the past decade. Conventionally, grey infrastructure (GR) is designed to

Abbreviations: CL-GR-GI, centralised Grey-Green infrastructure; CL-GR, centralised grey infrastructure; GR-GI, Grey-Green infrastructure; DL-GR-GI, decentralised Grey-Green infrastructure; DL-GR, decentralised grey infrastructure; GA, genetic algorithm; GCM, Global Climate Model; GI, green infrastructure; GR, grey infrastructure; LCC, life cycle cost; O&M, operation and maintenance; PV, present value; RCPs, Representative Concentration Pathways; RCM, Regional Climate Model; SWMM, Storm Water Management Model; TSS, total suspended substance.

* Corresponding author at: School of Design and Environment, National University of Singapore, 117356, Singapore.

E-mail address: jindaqi@nus.edu.sg (J. Qi).

<https://doi.org/10.1016/j.watres.2023.119720>

Received 13 August 2022; Received in revised form 22 January 2023; Accepted 4 February 2023

Available online 8 February 2023

0043-1354/© 2023 Elsevier Ltd. All rights reserved.

intercept, collect and channel the runoff for effective drainage. However, GR had the side effect of concentrating non-point source pollutants in the catchment area, resulting in extensive deterioration of the water quality of the recipient water body (Nika et al., 2020; Wang et al., 2021a). Comparatively, green infrastructure (GI) with natural-based solutions, including Low Impact Development, Water Sensitive Cities, Sustainable Urban Drainage Systems, and Sponge City could counter the pollution issues (Fletcher et al., 2015; Ying et al., 2021). These GIs are typically incorporated in decentralised structural practices, and manage the surface runoff at the source. As they are typically designed to mimic the natural hydrological condition before urbanisation, and are aesthetically pleasing, GIs could be strategically integrated as part of the urban stormwater management scheme and the city's development plan (McFarland et al., 2019; Nickel et al., 2014; Versini et al., 2018). Although the advantages of these strategies have been widely discussed and accepted, GI is recognized as being appropriate for stormwater management for rainfall of short return periods and in many cases cannot replace the role of GR, especially in the case of densely built-up urban environments (Xu et al., 2019). In such an urban environment, over 60% of the land surface is occupied by pavements and roofs and is drained through grey infrastructures (Qi et al., 2019). The remaining open space limits the scope and hydrological capacity of GI in response to extreme storms. For example, Mei et al. (2018) assessed 15 GI scenarios subject to rainfall with return periods of 2–100 years in Beijing, China, and concluded that the hydrological performance of the GIs was not satisfactory and could not eliminate urban flooding even for the case of the most optimistic scenario. Although GI can benefit stormwater management in multiple ways, including water quality, volumes and frequency of runoff, and floods, one should not expect to achieve high performance in flooding mitigation, particularly for long return periods, by just applying GI only.

GR and GI could be integrated appropriately and applied as potential advanced solutions for urban stormwater management (Browder et al., 2019). The integrated system leverages on the versatility and ecological aspects of GI and the engineering reliability and practicability of GR (Wang et al., 2021d, 2017b; Yang and Zhang, 2021; Zhou et al., 2022). To date, several integration schemes have been reported and they include the Grey-Green infrastructure (GR-GI) system to reduce the life cycle cost (LCC) (Bakhshipour et al., 2019a); the System for Urban Stormwater Treatment and Analysis Integration to evaluate the optimal location, type, and cost of stormwater best management practices (Lee et al., 2012); and integrated GR and low impact development to measure the technical and operational resilience of best management practices (Wang et al., 2021c). Other reported works include assessment of hydraulic reliability and hydrological resilience based on the selected rainfall events instead of continuous rainfall time series (Da Silva et al., 2018; Mohanty et al., 2020; Sohn et al., 2019; Wang et al., 2020). A long-term time series analysis for urban stormwater management would have considered multiple climatic variables, such as rainfall, intensity, duration, and antecedent dry days, to mention a few, as these parameters could influence the generation of runoff in the catchment, soil water storage capacity of the underlying surface, and source-accumulation process of non-point source pollutants (Madarang and Kang, 2013; Rossman and Huber, 2016; Salim et al., 2019). In adopting a single climatic variable (e.g., rainfall intensity) the hydrologic performance of the integrated GR-GI drainage system may be overestimated under certain hydrological conditions (Yu et al., 2022), not to mention the inherent limitation of using one single parameter to optimise the location, type, and cost of urban drainage systems for long-term applications.

Recently, climate models have also been used to assess the hydraulic performance of the GR or GI under various climate scenarios, such as Representative Concentration Pathways (RCPs), to help understand better the potential impact of design/planning decisions on urban hydrology. Zeng et al. (2021) evaluated the performance of GI in runoff quantity control and water quality improvement under RCP4.5 and

RCP8.5 scenarios (total radiative forcing topped at a stable 4.5 W/m² and 8.5 W/m², respectively, by 2100 at the grid-scale, see Meinshausen et al. (2011)). El-Housni et al. (2019) made projection of the hydraulic performance of the urban pipe network (2041 to 2070) based on the simulation results of the Canadian Regional Climate Model. However, the majority of the reported studies assessed and optimised the adaptive capacity of GR and GI in response to stationary or event-based climate scenarios, neglecting the effects of non-stationarity and nonlinearity of long-term climate change. Since climate change is dynamic and nonlinear, optimising the synergistic effects of GR and GI as the means to adapt to non-stationary climate change needs to be addressed urgently.

The relevant long-term time series parameters are readily influenced by climate change. For example, Noor et al. (2022) reported potential projected changes in rainfall intensity, attributable to climate change, of –3.4 – 26.7% (2010–2039), –0.1 – 34.5% (2040–2069) and –4.3 – 96.8% (2070–2099) from that observed during the base period (1971–2000). Therefore, forecasting reliable long-term time series data under various climate changes is also a vital component for accurate GR-GI optimisation. Global Climate Model (GCM) could be used to simulate the data of air temperature, precipitation, and atmospheric circulation on a global scale, and is considered to be an essential tool for the projection of climate change (IPCC, 2014; O'Neill et al., 2016). However, the GCM is appropriate at a large scale, due to certain defects and uncertainties of simulation data in geographic space (Willems et al., 2012). Regional Climate Model (RCM), a downscaling model driven by output from a GCM, can be applied to capture topographic and surface characteristics at local minor scales, as well as deviations of boundary conditions, providing parameterisation with observed cumulus, which in turn facilitated better simulation of extreme rainfall events (Giorgi and Mearns, 1999). RegCM4.6 (a common RCM) developed by the National center for Atmospheric Research and Pennsylvania State University has been used to perform bias correction on each grid point and showed high reliability and excellent predictive effect (Gao et al., 2017; Pan et al., 2020; Zhang et al., 2021). Several studies had made use of these models to perform comparative study of the results of present and future scenarios. However, only a handful of studies highlighted the dynamic changes in the climate change process (Yu et al., 2022). To better capture the dynamic changes, some researchers proposed using the Bernaola-Galván algorithm to identify mutation information in long-term time series data. The Bernaola-Galván algorithm is a segmentation algorithm originally used to “probe the temporal organisation of heterogeneities in human heartbeat interval time series” (Bernaola-Galván et al., 2001). Since the algorithm could be used to detect mutations in the climate change process, it might also be used to capture nonlinear and non-stationary climate change information (Chen et al., 2019; Jehanzaib et al., 2020; Yu et al., 2022), and provide insights on parameters at various stages of climate change. Hence, knowing the temporal variation or time series of the climate change, one would also be able to establish the time series of the various parameters. In short, both simulation models and segmented time series are crucial to obtaining realistic and reliable long-term time series parameters for accurately assessing and optimizing the GR-GI performance under various climate change scenarios since the performance varies significantly across the time series parameters, such as precipitation amount, intensity and interval time.

This paper presents a novel assessment framework to support the selection of GR-GI based on long-term time series information in tandem with non-stationary climate change. The specific objectives are: (1) to integrate RegCM 4.6 and Bernaola-Galván algorithm into establishing the long-term time series of parameters in tandem with non-stationary climate changes. The time series will be used to test the optimised GR-GI design and configuration; (2) to optimise the life cycle cost and hydrological performance of GR-GI using the graph-theory-based algorithm and genetic algorithm (GA); and (3) to optimise GR-GI under various climate scenarios in Guangzhou, China.

2. Methodology

The developmental framework consists of three parts (Fig. 1): (1) Assess and process the climate information to establish the appropriate climate change time series; (2) establish the optimal drainage design strategy; and (3) evaluate the hydrological performance of the drainage system in response to climate change. The long-term time series of precipitation is obtained by using dynamic downscaling of RegCM based on two RCPs. As for the spatial configuration of urban stormwater infrastructure, the optimal strategies at various levels of decentralised layouts are obtained through integrating graph theory and genetic algorithms. Then the hydrological performance of the recommended strategies for various representative climate change scenarios is evaluated using a hydrological model.

2.1. Case study

Guangzhou is located at the Pearl River Basin and has a subtropical

monsoon climate. The mean annual precipitation is about 1700 mm but the rainfalls are non-uniformly distributed. Also, Guangzhou is one of the cities with the most waterlogged and severe flood risk amongst 136 large coastal cities (Hallegatte et al., 2013). Covering an area of 101.8 hectares, Zhujiang New Town (Fig. 2) is the most prominent central business district in Guangzhou, and has the typical characteristics of a densely built-up city such as high impervious surface, high population density, and highly developed economy. This study selected Zhujiang New Town as the case study area. Zhujiang New Town consists of 43 sub-catchments. The Storm Water Management Model (SWMM), an open-access hydrological model developed by United States Environmental Protection Agency, was used to simulate the surface runoff, peak flow, and the total suspended solids (TSS) in an urban catchment (Rossman, 2010). The parameters of the sub-catchments in SWMM were obtained from the Wang et al. (2021c), and are listed in Table S1. The dynamic wave approach was used for the network confluence computation model, and the Horton model was used to describe the infiltration process. Appropriate saturation and exponential function were adopted

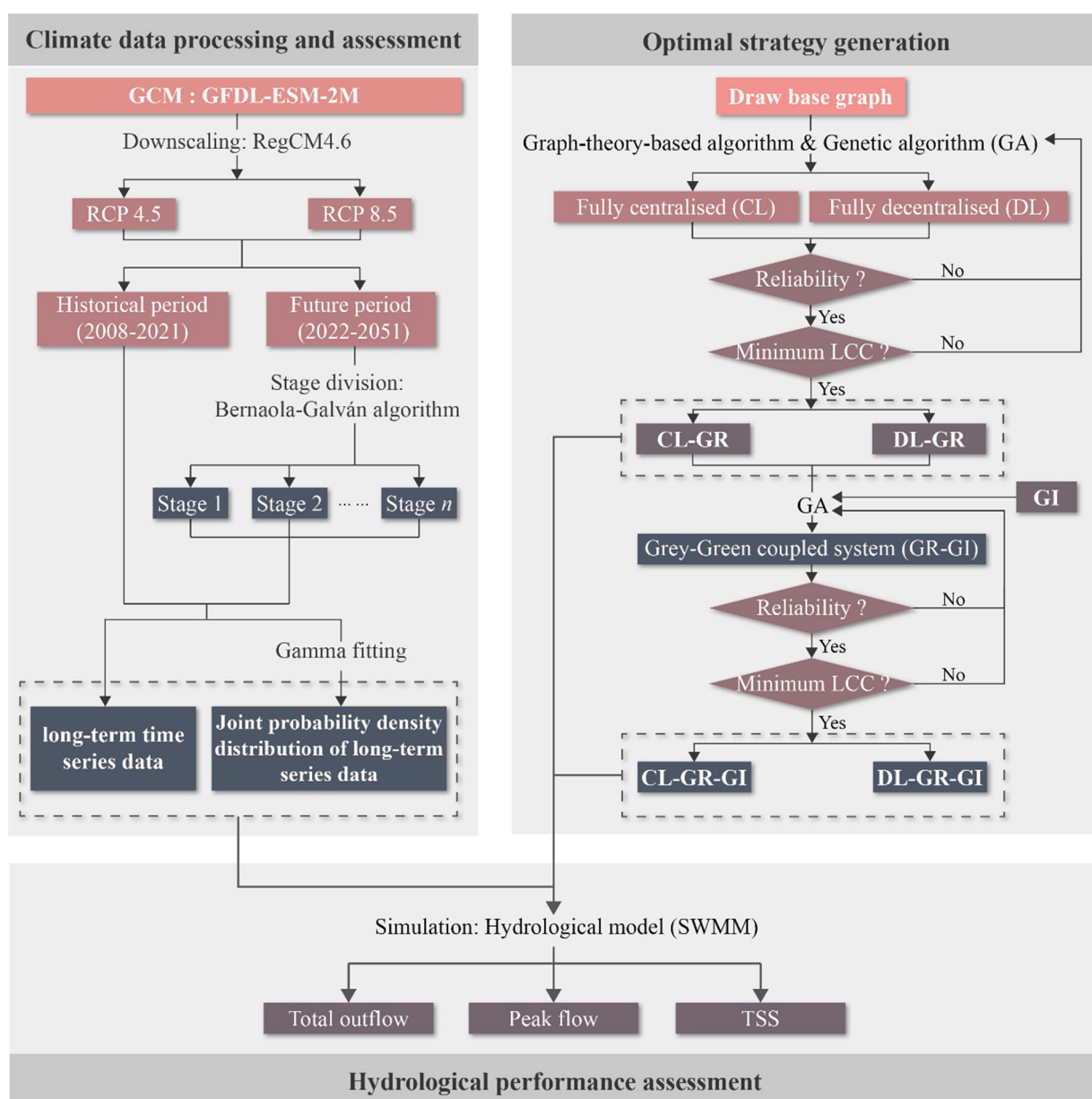


Fig. 1. The framework for hydrological assessment of the optimal GR-GI at various levels of decentralised layouts. Note: GCM - Global Climate Model; LCC - life cycle cost; GR - grey infrastructure; GI - green infrastructure; and TSS - total suspended substance.

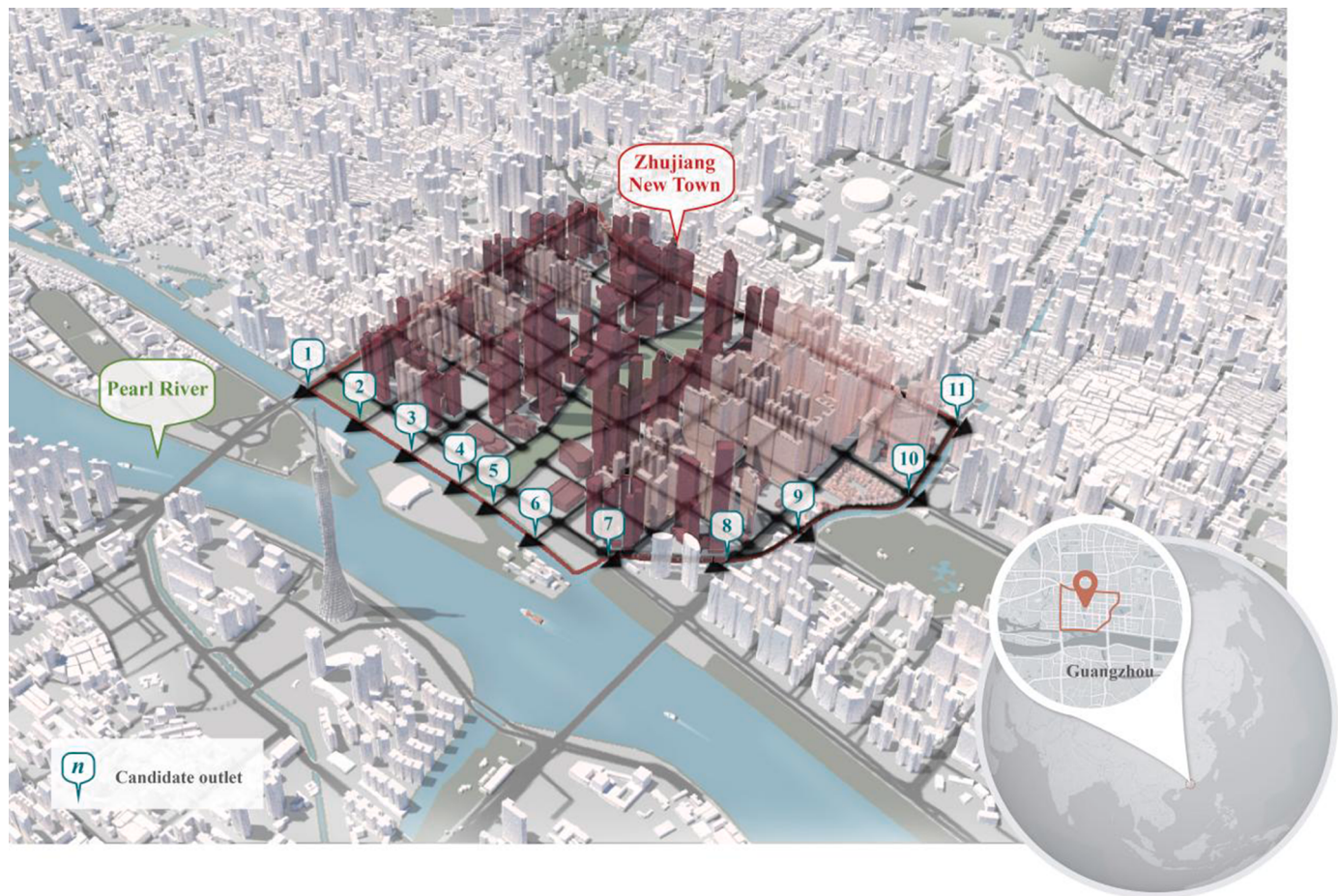


Fig. 2. The case study area – Zhujiang New Town in Guangzhou, China.

for pollutant accumulation and the wash-off model, respectively.

2.2. Climate information - processing and assessment

2.2.1. Climate data simulation

GFDL-ESM-2 M, which had been found to perform well for the Pearl River Basin of China (Zhang et al., 2021), was chosen to simulate climate data in this study. The simulation results were used as the initial and lateral boundary conditions for climate projection in this study. RegCM4.6 was adopted for dynamic downscaling ($0.25^\circ \times 0.25^\circ$). RCP4.5 and RCP8.5 were selected as climate scenarios as they may be used to represent similar intermediate and extreme scenarios for climate change, respectively, and had been widely utilised and reported in many studies (Requena et al., 2019; Yu et al., 2022; Zeng et al., 2021). The base period (2008–2021) was used, and for a 30-year life cycle of the coupled GR-GI system, the target future period was set for 2022–2051.

2.2.2. Managing the time series – stage division of data

Climate change is a change process with phase regularity. Reliable assessment of the projected climate changes is helpful to identify and explore the effects of meteorological factors on the performance of Grey-Green coupled strategy. The Bernaola-Galván algorithm has often been used to identify mutation information in long-term time series and has been found applicable to nonlinear and non-stationary climate change information (Chen et al., 2019; Jehanzaib et al., 2020; Yu et al., 2022). In this study, the Bernaola-Galván algorithm was chosen for stage division of the future period. It should be noted that before applying the Bernaola-Galván algorithm, an Augmented Dickey-Fuller test is required to verify the non-stationarity of the time series to be sub-divided

(Dickey and Fuller, 1979). The Augmented Dickey-Fuller is used to test a time series by detecting the existence of unit root in a time series sample, so as to ensure that the premise of Bernaola-Galván algorithm is met. The corresponding procedures of applying Bernaola-Galván algorithm are included in the annex (Text S1).

2.2.3. Data extraction and analysis

Three sets of data: precipitation, duration, and antecedent dry days have been found significant and relevant in the generation and analysis of climate change time series for the purpose of drainage design (Gong et al., 2016; Rasheed et al., 2019; Sohn et al., 2019). They were extracted from the simulated long-term time series. A rainfall event is defined as one with a rainfall depth exceeding 1 mm, and the minimum interval between two rainfall events is 6 hr or more (Joo et al., 2014). The probability density function used to describe the variation and distribution of rainfall is based on a two-parameter gamma distribution (Chapman, 1997) (Eq. (1)).

$$f(x) = \frac{x^{\alpha-1} e^{-\frac{x}{\beta}}}{\beta^\alpha \Gamma(\alpha)} \quad (1)$$

where $\alpha = \frac{\mu^2}{\sigma^2}$ is the shape parameter, $\beta = \frac{\sigma^2}{\mu}$ is the scale parameter, and μ is the mean value of the precipitation, duration or antecedent dry days series and σ is the variance.

The joint probability distribution function may be used for fitting the distribution relationship of the two factors (Yu et al., 2022), contributing to observing the distribution of precipitation with duration and antecedent dry days from a broader dimension (Eq. (2)).

$$f(x,y) = f(x)f(y) = \frac{x^{\alpha_x-1}y^{\alpha_y-1}e^{\frac{-x}{\beta_x}+\frac{-y}{\beta_y}}}{\beta_x^{\alpha_x}\beta_y^{\alpha_y}\Gamma(\alpha_x)\Gamma(\alpha_y)} \quad (2)$$

where $f(x,y)$ is the joint probability distribution of the precipitation and duration, or precipitation and antecedent dry days, where $f(x)$ is the gamma distribution of precipitation, and $f(y)$ is the gamma distribution of duration or antecedent dry days.

The joint probability density distribution of long-term time series was employed to assess the characteristics of climate change in different stages under various climate scenarios.

2.3. Optimal strategy development

2.3.1. Optimisation objectives and constraints

In general, the calculation function used for searching the optimal minimum-cost of a coupled system is expressed as Wang et al. (2021c):

$$d_{\text{opt}} = \underset{d \in D}{\operatorname{argmin}} [f_{\text{cost}}] \quad (3)$$

where, d is the decision variable; D represents all feasible plans for the system; and d_{opt} is the optimal solution. When GI is included in the optimisation, d may be extended as Eq. (4):

$$d = [DDL, \text{layout parameters}, \text{hydraulic parameters}, \text{GI parameters}] \quad (4)$$

where, the decision variable d contains the degree of decentralisation of the drainage layout (DDL), layout parameters (i.e., connections between different sewers), hydraulic parameters (i.e., pipe diameters and slopes that satisfy the hydraulic constraints), and GI parameters of the coupled system (type, size, and location of GI).

To characterise the minimum-cost quantitatively, LCC expressed in present value (PV), is an important indicator of the capital urban infrastructure investment, and operation and maintenance (O&M) cost of the infrastructure Chui et al., 2016; Dos Santos et al., 2021). The optimal strategies at various levels of decentralised layouts for the least LCC is expressed as Eqs. (5) and (6):

$$LCC = Capital_{\text{Infrastructure}} + PV_{O\&M-\text{Infrastructure}} \quad (5)$$

$$PV_{O\&M-\text{Infrastructure}} = \sum_1^n O\&M \frac{1}{(1+i)^n} \quad (6)$$

where, $PV_{O\&M}$ is the PV cost of O&M during the life span; i is the discount rate, which is taken as 2% (Dong, 2018); n is the lifespan, and which is taken as 30 years according to Xu et al. (2017). In this study, the capital costs were calculated based on local engineering market, and the annual O&M costs of GR and GI in Guangzhou were taken as 10% and 8% of the capital cost, respectively, according to Houle et al. (2013).

In addition, we include hydraulic reliability as a constraint in the optimisation process according to local outdoor drainage design standards (MHURD, 2016), that is, no flooding occurred following the design rainfall. The design rainfall selected was a 5-yr return period and 6-hr duration, which was 121 mm rainfall depth in Guangzhou. The internal characteristics followed that of a Chicago hyetograph. The current engineering practice is such that the design of GR is based on a specific design rainfall (certain return period and duration). The performance of the so designed infrastructure is subsequently in the assessment of the overall system subject to certain selected events. There are obvious advantages to evaluate the system performance based on a series of events, and the ultimate test would be based on a time series of hydrological and climate change incorporating various relevant parameters. Given the nature of the hydrological and climate change events, the list of parameters would be large and almost always "not exhaustive enough" to describe all aspects of the change. We discovered that an exorbitant amount of computation hardware and software resources is required to perform optimisation for discrete events with a short list of carefully selected parameters. Using a time series of selected

parameters would be hard put given our available resources. After much deliberation, we compromised by adopting an alternative approach in the formulation of the algorithm, and had chosen to use certain discrete design rainfall event for the optimisation instead.

2.3.2. GR strategy optimisation

Initially, the spatial configuration algorithm based on a graph theory is utilised to search for various decentralised layouts of GR, that is expected to provide suitable and hydraulically adequate basic networks for GR-GI (Bakhshipour et al., 2019a). This algorithm can generate all possible sewer spatial configurations with various degrees of decentralisation from a base plan (drainage network follows the street alignments). It is a connected cyclic graph that includes all drainage possibilities. In the base plan, vertices represent manholes and edges joining the vertices represent sewers. According to Bakhshipour et al. (2019a), the first step is to define the degree of decentralisation of the layout, which is determined by the number of selected and candidate outlets across the system:

$$DDL = \frac{N_{SO} - 1}{N_{CO} - 1} \times 100\% \quad (7)$$

where N_{SO} denotes the selected number of outlets, and N_{CO} represents the total number of candidate outlets. The main objective of the study is to develop a replicable approach for the assessment of GR-GI in response to non-stationary climate change and demonstrate its feasibility and application. Either fully centralised, i.e., $DDL=0\%$, and fully decentralised network, $DDL=100\%$ are investigated in this study.

The optimisation process follows: first a fully centralised layout is selected (only one outlet out of N_{CO} possible outlets). This is the fully centralised network (CL-GR). Then a second outlet from the remaining $(N_{CO} - 1)$ outlets is selected randomly and added to the first network. Including a second outlet means that the first network would be partitioned to form two sub-networks, each discharges through the respective outlet. The configuration of the sub-network is selected by using the algorithm which uses graph theory to assign different parts of the network to different outlets and generates the decentralised layout. Then the process is repeated by adding a third, fourth, and fifth outlets etc. until all N_{CO} outlets are included, and the corresponding sub-networks were configured using the above mentioned algorithm. The algorithm needs $2 \times N_s$ decision variables to generate one feasible layout. N_s is the number of sub-catchments in the base graph. After generating the layout, the size of the GR network components (e.g., pipe diameters and manholes invert elevation) must be designed in such a way that satisfies all hydraulic and technical criteria. For this purpose, the adaptive sewer design algorithm introduced by Haghghi and Bakhshipour (2012) was adopted in this study. The constraints are the telescopic pattern of sewer diameters, minimum and maximum cover depths, slopes, flow velocity and hydraulic reliability. Each alternative layout requires $2 \times N_p$ decision variables in the genetic algorithm; here N_p represents the total number of pipes. For each pipe, one variable determines the pipe's diameter, and other one determines pipe's slope (by adjusting the invert level of the manhole). Therefore, the total number of decision variables for GR strategy and optimisation (generating a decentralised layout and sizing it) is $2 \times (N_p + N_s)$.

2.3.3. Grey-Green infrastructure system optimisation

Considerable investment is required to construct and maintain the conventional GR, and the introduction of GI may somewhat decrease the construction demand for GR, and thus reduce the investment as the cost for construction and maintenance of GR-GI is relatively lower (Wang et al., 2021c). The general constraints for configuring a Grey-Green infrastructure system include the street network (the sewer pipe runs parallel and at the side of the streets), ground elevation, obstacles, distance of recipient water body from the outlet(s), and space available for the construction. Moreover, considering the actual construction are

located in a high-density city space, the construction scale of GI needs to be controlled to no larger than 10% of the sub-catchment areas (Eckart et al., 2017).

Being one of the most popular types of GI, a bioretention cell comprises surface vegetation, graded soil, pore space storage, and underground drainage layers, and is widely and flexibly used in high-density cities where open space is scarce (Lim and Lu, 2016; Wang et al., 2021b). For most practical purposes bioretention cells are mainly designed to reduce the amount and delay the flow of surface runoff, remove non-point source pollutants, and beautify the environment (Liu et al., 2015). The parameters of the bioretention cell module in SWMM can be found in Table S2.

After optimising GR networks as explained in Section 2.3.2, GI can be introduced to the system to formulate coupled GR-GI configuration. Here, a binary system is used to annotate GA that is utilised to optimise the coupled system and hence determine the minimum LCC (Ene et al., 2016). In this process, the decision variables are encoded as binary values (i.e., 0 and 1), and a “chromosome-equivalent” composed of these values is used to represent one design scheme (Hsu et al., 2005). In the present study, there are N_S (number of sub-catchments) + $2N_P$ (number of pipes) values in each chromosome to reflect the decision variables, where N_S values control GI in each sub-catchment i and each value is decoded as follow:

$$GI_i = \begin{cases} 1 \rightarrow \text{Subcatchment } i \text{ has GI} \\ 0 \rightarrow \text{Subcatchment } i \text{ has no GI} \end{cases} \quad (8)$$

As GI is introduced into the GR layout, the GR diameter could be and will be reduced to achieve minimum LCC, while hydraulic reliability is held at the same level as before. The pipe diameter (D) will be controlled by $2N_P$ values, represented by a two bits code and define the relative diameter of a pipe (j):

$$D_j = \begin{cases} 11 \rightarrow D = \text{Same as in the GR scheme} \\ 10 \rightarrow D = \text{One size smaller than in the GR scheme} \\ 01 \rightarrow D = \text{Two sizes smaller than in the GR scheme} \\ 00 \rightarrow D = \text{Three sizes smaller than in the GR scheme} \end{cases} \quad (9)$$

To obtain the minimum cost configuration, these pipe diameters need to be iterated through GA to minimize the LCC. Finally, the centralised Grey-Green infrastructure (CL-GR-GI) system and decentralised Grey-Green infrastructure (DL-GR-GI) system alternatives are generated based on the two optimal GR layouts (centralised and fully decentralised) with the corresponding DDL.

2.4. Hydrological performance assessment

The ability to control water quantity and quality are two critical aspects of urban stormwater system assessment (Islam et al., 2021; Rezaei et al., 2021). As for water quantity, the reducing ratios of total outflow and peak flow were chosen as the indicators in this study, which had been used hydrological performance assessment (Gong et al., 2019; Jiang et al., 2017; Xing et al., 2016). Here, total outflow refers to the full amount of the final outflow from the end of the network (sum of all outlet flow); and peak flow refers to the maximum outflow from the end of the drainage system over the whole period.

The strategy with the highest cost amongst the four optimised strategies was taken as the benchmark. The ratios of the total outflow and peak flow relative to the corresponding values for the benchmark, were used as evaluation indexes for the optimised strategy, and the expressions are as follows:

$$TO_n = \left(1 - \frac{V_{total_n}}{V_{total_{Benchmark}}} \right) \times 100\% \quad (10)$$

$$RP_n = \left(1 - \frac{V_{peak_n}}{V_{peak_{Benchmark}}} \right) \times 100\% \quad (11)$$

where TO_n and RP_n are the ratios of total outflow and peak flow, respectively; Similarly, the total suspended solids (TSS), a reflection of water quality in the recipient water body (Bilotta and Brazier, 2008; Wang et al., 2018, 2017a) may be treated in the same manner:

$$RT_n = \frac{M_{Removal}}{M_{Buildup}} \times 100\% \quad (12)$$

where, RT_n is the removal rate of TSS, and $M_{removal}$ and $M_{bulidup}$ present the removed and accumulated mass of TSS, respectively.

3. Results and discussion

3.1. Climate simulation results

RCP4.5 and RCP8.5 from 2008 to 2051 were adopted to represent the annual precipitation for the two scenarios. Both time series showed upward rising trend, and the upward trend of RCP8.5 (coefficient of variation = 0.3) was more prominent than that of RCP4.5 (Fig. 3a and 3b). These characteristics were consistent with the local future rainfall predictions (Wu and Huang, 2016; Zhang et al., 2021). Compared with RCP8.5, more events were observed in RCP4.5, and showed higher amount and intensity of rainfall (Fig. 3c).

Based on the results of the Augmented Dickey-Fuller test, the long-term series data were shown to be non-stationary ($P = 0.768$). The Bernaola-Galván algorithm was also used to identify the nodes between the prediction stages (2022–2051). Based on RCP4.5, the future meteorological stage was sub-divided into two stages: stage 1 (2022–2028, $n = 977$) and stage 2 (2029–2051, $n = 3187$); In the case of RCP8.5, the two stages were 2022–2031 ($n = 1161$) and 2032–2051 ($n = 2225$). Even though the RCP8.5 scenario contained less rainfall, the annual average rainfall increased more than those of the base period (7% in stage 1 and 17% in stage 2).

Based on the statistics of independent events obtained (Table 1), an average rainfall event during stage 1 in RCP4.5 was 13.9 mm, while the average in stage 2 was 15.0 mm, while the independent rainfall in RCP8.5 remained at about 8.7 mm on average. In terms of rainfall duration, each stage in RCP4.5 remained at about 13.0 h, while the corresponding duration for each stage of RCP8.5 was close to 10 h. The longer rainfall duration means higher probability of higher rainfall amount. One may conclude that the frequency of rainstorms was higher based on the RCP4.5 scenario. Furthermore, the frequency for rainfall exceeding 50 mm increased from 4.7% observed during the base period to 6.3% in stage 2, and the frequency of rainfall exceeding 100 mm increases from 1.6% observed during the base period to 2.3% in stage 2. A downward trend in the frequency of heavy storms in RCP8.5 was observed. It can be seen in Table 1 that the frequency for rainfall exceeding 50 mm decreases from 2.2% observed during the base period to 1.7% in stage 2, and the frequency of rainfall exceeding 100 mm decreases from 0.5% observed during the base period to 0.4% in stage 2. Significant changes of antecedent dry days were observed in RCP8.5, indicating a more frequent arid climate. Compared to that observed during the base period, the antecedent dry days of stage 1 and stage 2 increased by 39.1% and 51.5%, respectively in RCP8.5, with the average antecedent dry days increased from 1.9 days to 2.9 days. The maximum antecedent dry days could reach 150 days. In contrast, the antecedent dry days of RCP4.5 were relatively constant, showing a mean of 2.1 days. This observation was in line with that reported by Wu and Huang (2016) and Shi et al. (2020).

The joint probability distributions of the precipitation amount and duration, and the precipitation amount and antecedent dry days are shown in Fig. 4. In the case of RCP4.5, most of the rainfall events which exceed 100 mm are accompanied by long duration (Fig. 4a). Thus, the overall rainfall intensity was not high. On the other hand, the duration of rainfall events was shorter in RCP8.5, indicating higher rainfall intensities, especially so for extreme rainfall events. Since urban waterlog

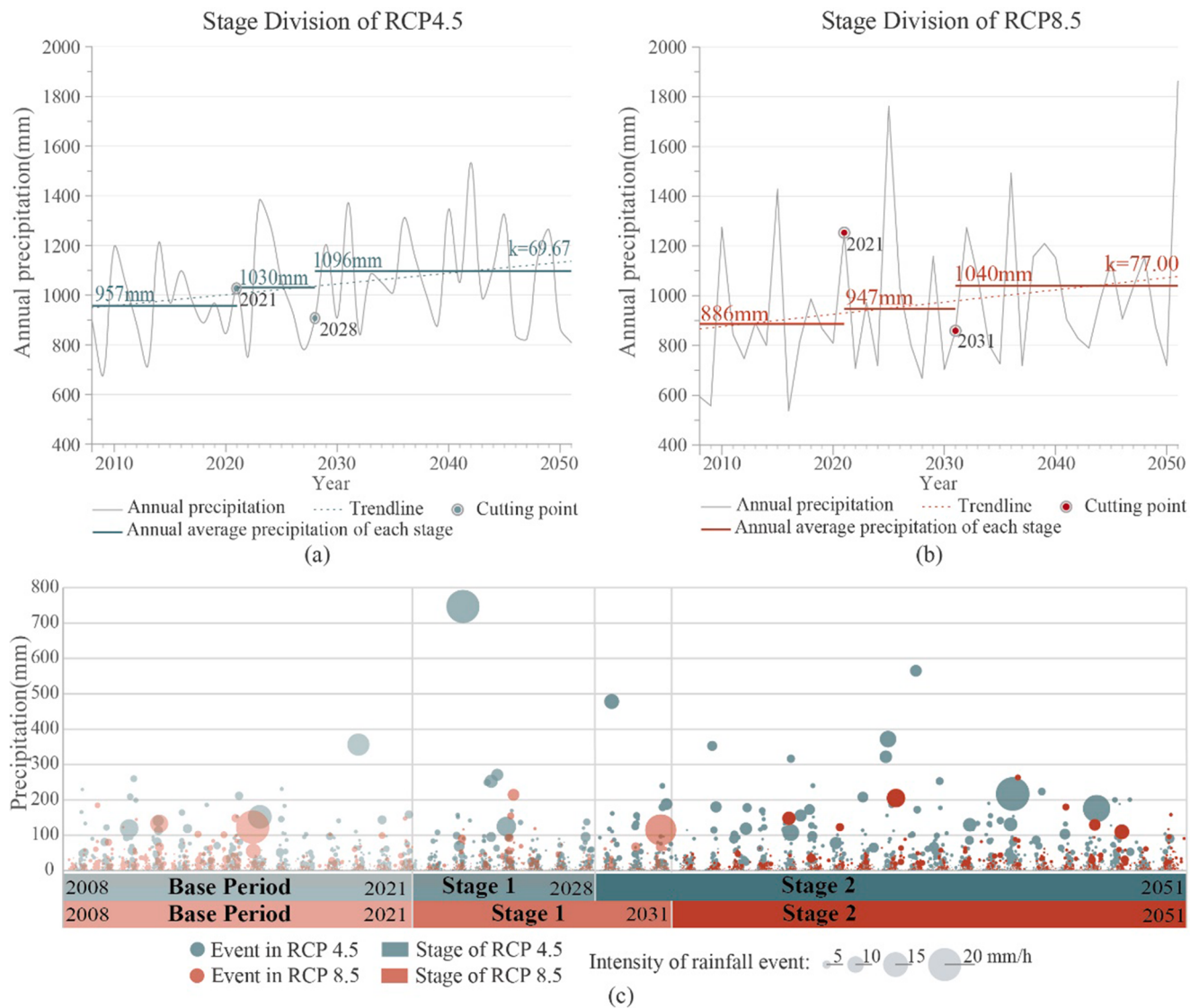


Fig. 3. Stage division and rainfall events abstraction. (a) Annual precipitation and stage division of RCP4.5, (b) Annual precipitation and stage division of RCP8.5; and (c) Distribution of rainfall events at various stages of selected scenarios.

Table 1

The statistics of climatic characteristics at each stage.

Climate change Scenarios		RCP4.5	Stage 1	Stage 2	RCP8.5	Stage 1	Stage 2
		Base Period			Base Period		
Average number of events per year		140	140 (-0.6%)	139 (-1.3%)	156	116 (-25.7%)	111 (-28.8%)
Antecedent dry days	Mean (days)	2.1	2.0 (-2.7%)	2.1 (+0.4%)	1.9	2.6 (+39.1%)	2.9 (+51.5%)
Precipitation	Max (days)	81.5	49.5 (-39.3%)	112.5 (+38.0%)	112.0	130.8 (+16.7%)	149.8 (+33.7%)
	Mean (mm)	12.8	13.9 (+8.3%)	15.0 (+17.1%)	8.1	8.0 (-1.9%)	8.0 (-2.4%)
	Max (mm)	353.4	740.3 (+109.5%)	560.1 (+58.5%)	184.0	213.9 (+16.3%)	262.7 (+42.8%)
	$x \leq 50\text{mm}$	n	134	132 (-1.2%)	130 (-3.0%)	153	113 (-25.8%)
		Ratio	95.3%	94.8% (-0.6%)	93.7% (-1.7%)	97.8%	97.6% (-0.2%)
	$50 < x \text{ mm}$	n	7	7 (-10.9%)	9 (+33.0%)	3	3 (-18.3%)
		Ratio	4.7%	5.2% (+11.6%)	6.3% (+34.8%)	2.2%	2.4% (+9.9%)
	$100 < x \text{ mm}$	n	2	2 (-16.1%)	3 (+43.3%)	1	1 (-30.0%)
		Ratio	1.6%	1.3% (-15.6%)	2.3% (+45.3%)	0.5%	0.4% (-5.8%)
Duration	Mean (h)	13.0	12.9 (-0.5%)	13.4 (+3.7%)	9.7	10.6 (+9.6%)	10.4 (+7.3%)
	Max (h)	132.0	102.0 (-22.7%)	156.0 (+18.2%)	78.0	84.0 (+7.7%)	84.0 (+7.7%)

is often triggered by rainstorms with high rainfall intensity, therefore, we focused on rainfall events with high precipitation (Fig. 4b). It is noted that high precipitation typically coincides with shorter antecedent dry days. From Fig. 4b, it can be seen that rainstorms are usually continuous

and intense in the study area, which is also consistent with the precipitation in the subtropical monsoon region. According to RCP8.5, antecedent dry days showed a longer duration and hence more frequent drought events. However, the antecedent dry days of extreme rainstorm

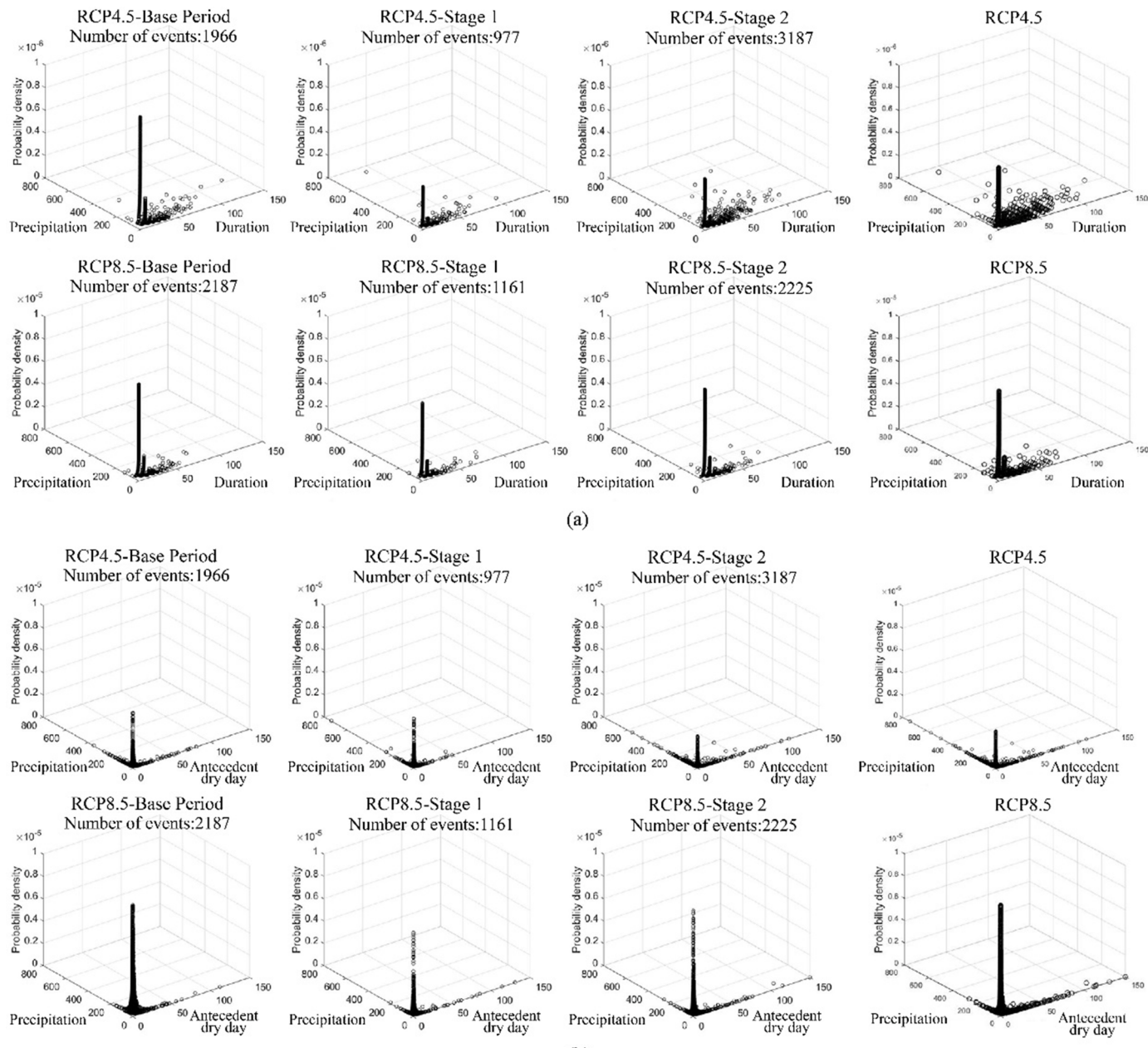


Fig. 4. The probability density distribution of rainfall events during various stages of RCP4.5 and RCP8.5. (a) the probability density distribution of precipitation and duration; and (b) the probability density distribution of precipitation and antecedent dry days.

events appeared an exception as the antecedent dry days were relatively small. Isolated rainstorm mode appeared not changed significantly.

3.2. Optimum drainage configuration

The optimised configuration of GR and GR-GI at various degrees of decentralisation are shown in Fig. 5. Each configuration were run through 320,000 iterations to obtain the optimum design, a process that took 30 h based on a PC equipped with Intel Core i5, 2.9 GHz dual-core CPU and 16 GB of RAM. Fig. 5 shows the pipe diameter and the corresponding pipe slope reflected as burial depth of the coupled system. The pipe diameters are significantly smaller than that designed for the single grey system. In the coupled system, the GI area in a fully centralised GR-GI (CL-GR-GI) accounts for 6.6% of the drainage area, while the area in a fully decentralised GR-GI (DL-GR-GI) accounts for 5.8% of the catchment area. A CL-GR-GI design contained a larger proportion of GIs. An

optimised coupled GR-GI system is more attractive than fully GR system in terms of the cost (Fig. 6). Specifically, it is clear that at the same degree of decentralisation, the LCC savings of a fully centralised and decentralised GR-GI systems are 18% and 11% compared to the fully GR system at the same degree of decentralisation, respectively. This observation also shows that GI has the potential of replacing a significant proportion of the centralised layout, and lead to significant cost reduction. Compared to a centralised GR-GI, the decentralised solution produced an additional 16.2% saving of the LCC. This is because of the relatively low cost associated with a highly decentralised layout (Wang et al., 2021c). It is also noted that large scale GI construction is typically not required, which further compresses the construction investment of the decentralised GR-GI. Therefore, an optimised and fully decentralised Grey-Green design is most economical and competitive while satisfying the hydraulic reliability requirement.

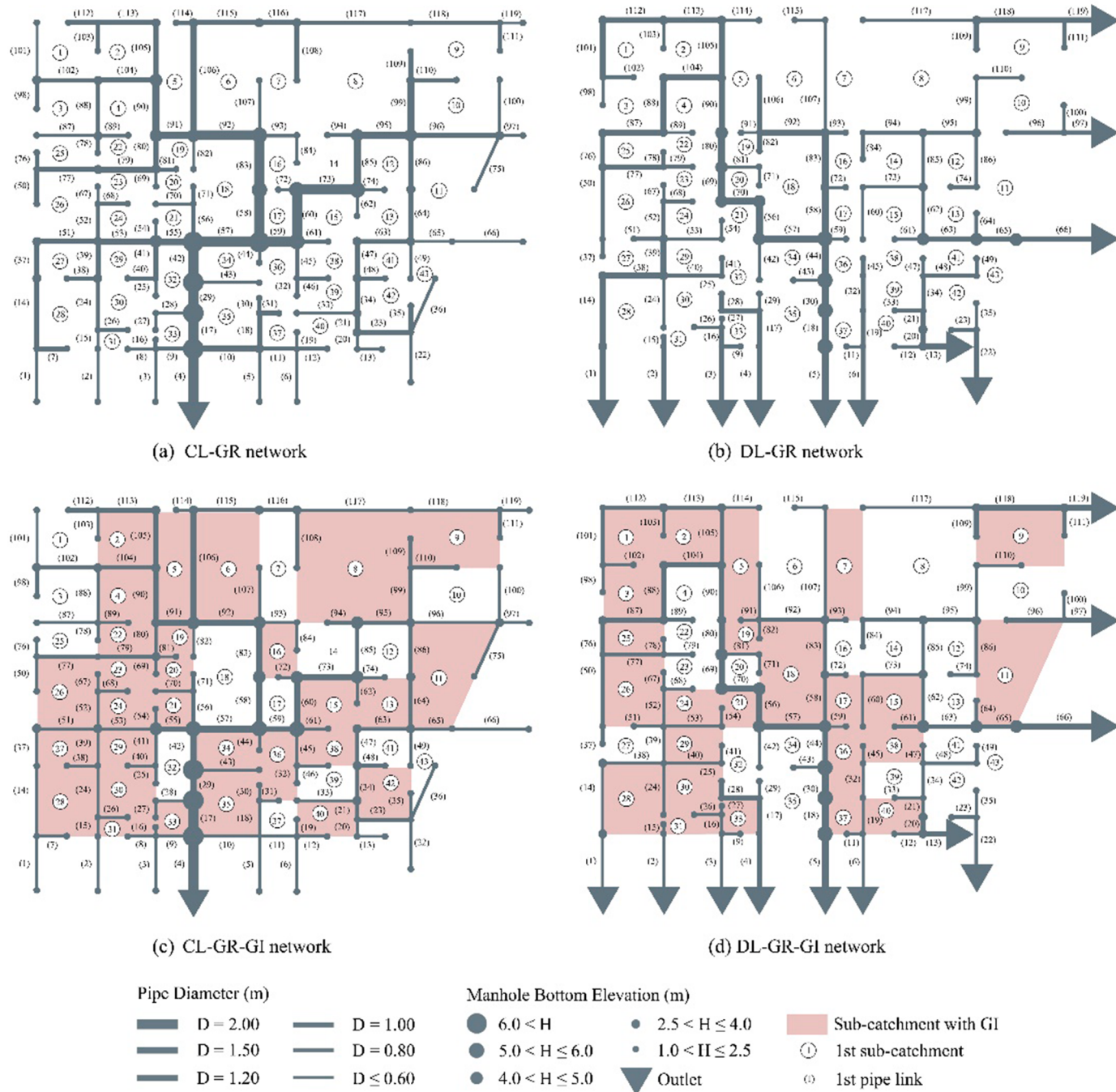


Fig. 5. Spatial allocation of optimised strategies (Wang et al., 2022): (a) the spatial allocation of optimised CL-GR; (b) the spatial allocation of optimised DL-GR; (c) the spatial allocation of optimised CL-GR-GI; and (d) the spatial allocation of optimised CL-GR-GI.

3.3. Hydrological performance

The hydrological performances of the optimised strategies were evaluated using a catchment-runoff model, SWMM, and included considerations of reducing the outflow, peak flow, and TSS. The simulation was calculated for 12 h simulation time.

Since the LCC of the centralised GR is the least ideal, it was used as a benchmark strategy to evaluate the systems' performance of runoff volume. Based on the findings of the simulation, it is found that, with regards to outflow discharge, GR-GIs could achieve reduction ratios of 56–66% (Fig. 7a). In terms of hydrological performance, the CL-GR-GI system scored the best. As a result of the configuration of larger-scale GI implemented in CL-GR-GI, most of the light rainfalls were effectively

retained at source, and the outflows were not affected significantly with climate change. This result demonstrates that as an annualised index, reduction of annual outflow is not sensitive with climate change. Similar results have been reported by Kim et al. (2018) and Yang and Zhang (2021).

Fig. 7b shows that DL-GR-GI achieved the most effective performance in reducing peak flow, with a score between 71% and 85%, which is significantly different from the outflow discharge. It is worth noting that the performance of decentralised GR was second only to DL-GR-GI and was significantly higher than CL-GR-GI. The reason is the strong role of decentralised networks in attenuating peak flow (Bakhshipour et al., 2019b; Wang et al., 2021c). There is also the added positive characteristics of a decentralised layout with multiple outlets which could

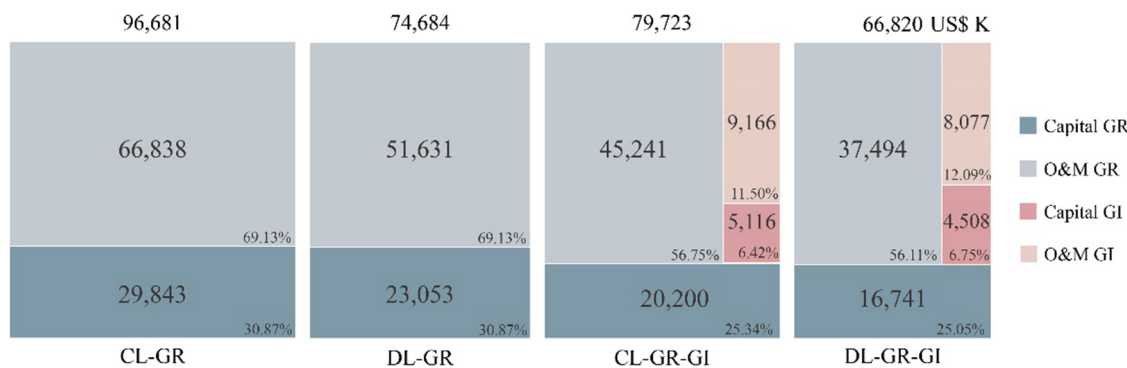


Fig. 6. Life cycle cost of various optimisation strategies (Wang et al., 2022).

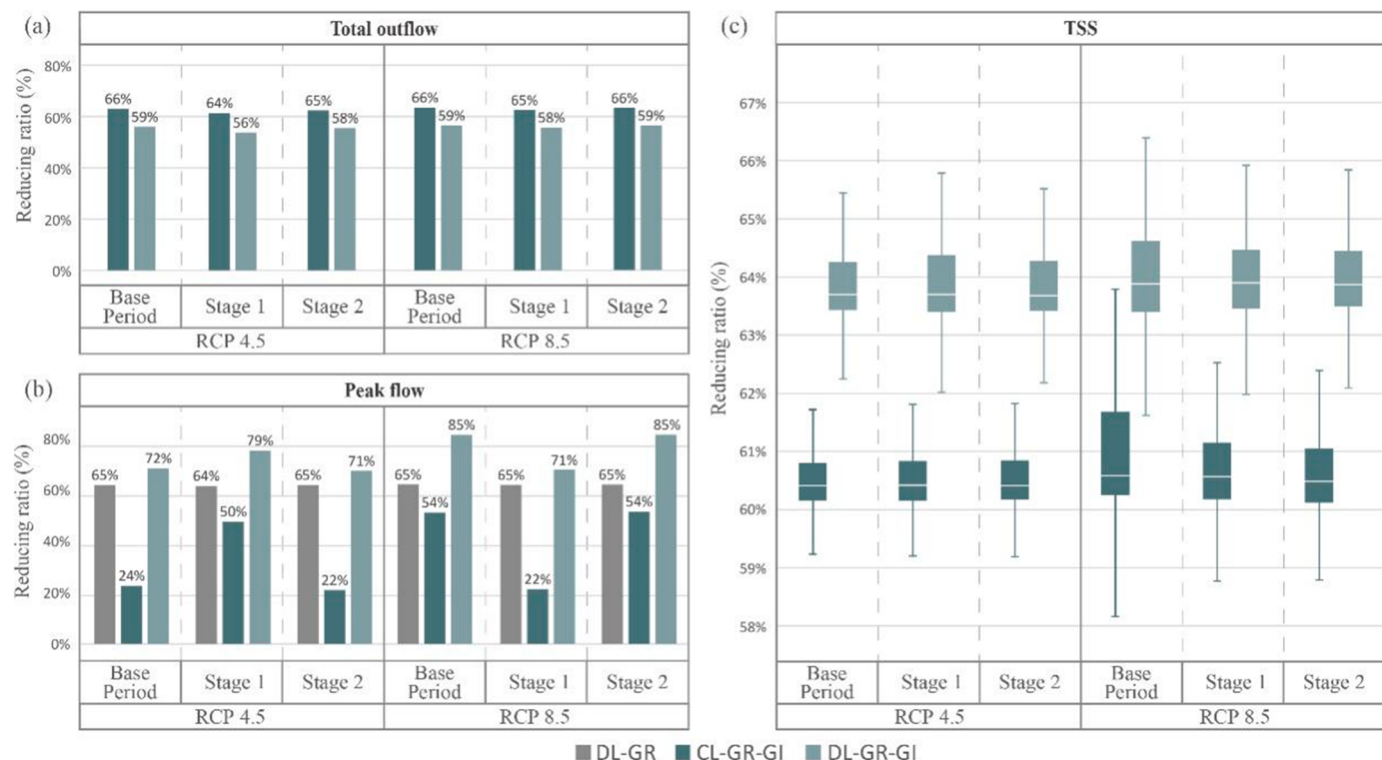


Fig. 7. Performance of long-term time series simulation of each strategy compared with CL-GR for each stage of RCP4.5 and RCP8.5. (a) The reducing ratios of total outflow; (b) The reducing ratios of peak flow; and (c) The reducing ratios of TSS.

effectively moderate the impacts of the discharge even when the storage capacity of GI is reached. Meanwhile, there is observed that peak flow reduction in DL-GR was generally maintained at 65% for various climate scenarios. In comparison, the capacity for peak flow reduction in the case of GR-GIs was highly sensitive to climate change. In the case of RCP4.5, the performance of GR-GI decreases to certain degrees from stage 1 to stage 2, and the reducing rate of CL-GR-GI decreases from 50% to 22%. This is primarily due to more intense extreme rainfall events being observed during stage 2. The hydrological performance of CL-GR-GI was less favourable as the GI portion of the drainage system does not perform well during extreme rainfall. Similar results have been obtained in studies of independence GI performance (Bae and Lee, 2020; Hu et al., 2019). The centralised layout lacks sufficient resilience, and GI is usually only used to manage runoff at source. When extreme events generate more runoff than the upper retention limit, GI basically fails to limit flood peaks (Zeng et al., 2021).

In terms of the removal rate of TSS, the GR-GIs depicted a rate of more than 60% (Fig. 7c), which is largely dependent on the pre-

retention property of GI on TSS. In GR-GI, the removal efficiency of TSS is unstable under RCP8.5. In RCP8.5, antecedent dry days are increased significantly, potentially results in increased TSS accumulation in the catchment. Consequently the removal efficiency of TSS in GR-GI would decrease. While a larger scale GI is anticipated to retain the TSS, intriguingly, the DL-GR-GI with lesser extent of GI was observed to show better performance in removing TSS. Plausibly the decentralised spatial topology may have increased the contact opportunities between runoff and GI, leading to better retention of TSS in the catchment.

3.4. Limitations and future work

Certain limitations of this study could be improved and carried out in future work. First, with the updating of GCMs, more possibilities for climate change have been proposed, which may not be able to be fully covered by a single climate model. In the future, the ensemble of multi-climate models can be considered to provide a varied and reliable prediction of the non-stationarity of future climate change and to achieve a

more reasonable layout optimisation. Second, the simulation process is time-consuming. An improvement of the optimisation algorithm could be carried out to refine the search for an optimum solution. Third, this study employed GA optimisation and focused on economic performance in the optimisation, which may not be comprehensive and adequate for addressing real-life applications with multiple objectives, such as more non-point source pollution indicators (e.g., Nitrogen compounds and Chemical Oxygen Demand). More advanced optimisation algorithms could be developed and used to tackle multi-objective problems in the future. Finally, the framework presented in this paper considered only bioretention cells as a GI example, and may not be universally applicable for GI allocation. Future applications could include more GI types to support comprehensive and universally applicable decision-making considerations.

4. Conclusions

A novel assessment framework for an urban Grey-Green infrastructure system is described in response to climate change. The current framework leverages the synergistic effect of GR and GI within a coupled drainage system to produce a superior hydrological performance at the least life cycle cost. It highlights the impacts of non-stationary time series rather than stationary or event-based climate scenarios emphasised in previous studies on GR-GI optimisation. Applying the framework to optimize GR-GI in Guangzhou, China, with respect to over 30 years of climate change shows that: First, compared to the conventional grey infrastructure drainage solution, the decentralised and centralised GR-GI are economically competitive with a saving of 11% and 18% of the whole life cycle cost compared with that of conventional GR, respectively; Second, the degree of decentralisation of GR-GI has higher impacts than the areal proportion of GI in GR-GI on hydrological and economic performance. The less extent of GI in a decentralised GR-GI depicted high performance in removing TSS in long-term time series simulations; Finally, the decentralised GR-GI shows superior performance in scenarios with extremely long antecedent dry days. Therefore, in addition to the factors of precipitation and rainfall duration, antecedent dry days should be taken into consideration to evaluate the impacts of climate change on optimised GR-GI strategies in a more comprehensive way. The assessment methods developed in this study have the potential to provide a reference for the planning and decision-making of GR-GI in high-density urban areas. The proposed framework can not only assess and optimize GR-GI under non-stationarity time series but also be a powerful support for stormwater management in response to climate change.

Declaration of Competing Interest

None.

Data availability

Data will be made available on request.

Acknowledgement

This work was supported by the National Natural Science Foundation of China [grant number 51808137], Natural Science Foundation of Guangdong Province [grant number 2019A1515010873], and Science and Technology Program of Guangzhou, China [grant number 202201010431].

Supplementary materials

Supplementary material associated with this article can be found, in the online version, at doi:10.1016/j.watres.2023.119720.

References

- Aerts, J.C.J.H., Botzen, W.J.W., Emanuel, K., Lin, N., de Moel, H., Michel-Kerjan, E.O., 2014. Evaluating flood resilience strategies for coastal megacities. *Science* 344 (6183), 472–474.
- Bae, C., Lee, D.K., 2020. Effects of low-impact development practices for flood events at the catchment scale in a highly developed urban area. *Int. J. Disast. Risk Res.* 44.
- Bakhshipour, A.E., Bakhshizadeh, M., Dittmer, U., Haghghi, A., Nowak, W., 2019a. Hanging gardens algorithm to generate decentralized layouts for the optimization of urban drainage systems. *J. Water Res. Plan. Man.* 145 (9).
- Bakhshipour, A.E., Dittmer, U., Haghghi, A., Nowak, W., 2019b. Hybrid green-blue-gray decentralized urban drainage systems design, a simulation-optimization framework. *J. Environ. Manage.* 249, 109364.
- Bernaola-Galván, P., Ivanov, P.C., Amaral, L.A.N., Stanley, H.E., 2001. Scale invariance in the nonstationarity of human heart rate. *Phys. Rev. Lett.* 87 (16), 168105.
- Bilotta, G.S., Brazier, R.E., 2008. Understanding the influence of suspended solids on water quality and aquatic biota. *Water Res.* 42 (12), 2849–2861.
- Browder, G., Ozment, S., Rehberger Bescos, I., Gartner, T., Lange, G.M., 2019. Integrating Green and Gray: Creating Next Generation Infrastructure. World Bank and World Resources Institute.
- Chapman, T.G., 1997. Stochastic models for daily rainfall in the Western Pacific. *Math. Comput. Simul.* 43 (3–6), 351–358.
- Chen, P., Tan, G.M., Deng, J.Y., Xu, Q.X., Tang, R.X., 2019. Mutation analysis of annual sediment discharge at Wu Long station in Wu Jiang River Basin from 1960 to 2016. *PLoS ONE* 14 (12), e0225935.
- Chui, T.F.M., Liu, X., Zhan, W.T., 2016. Assessing cost-effectiveness of specific LID practice designs in response to large storm events. *J. Hydrol.* 533, 353–364.
- Da Silva, C.V.F., Schardong, A., Garcia, J.I.B., Oliveira, C.D.M., 2018. Climate change impacts and flood control measures for highly developed urban watersheds. *Water-Sui* 10 (7).
- Dickey, D.A., Fuller, W.A., 1979. Distribution of the estimators for autoregressive time series with a unit root. *J. Am. Stat. Assoc.* 74 (366a), 427–431.
- Dong, Y., 2018. Performance assessment and design of ultra-high performance concrete (UHPC) structures incorporating life-cycle cost and environmental impacts. *Constr. Build. Mater.* 167, 414–425.
- Dos Santos, M.F.N., Barbassa, P., Vasconcelos, A.F., 2021. Low impact development strategies for a low-income settlement: balancing flood protection and life cycle costs in Brazil. *Sustain. Cities. Soc.* 65.
- Eckart, K., McPhee, Z., Bolisetti, T., 2017. Performance and implementation of low impact development – a review. *Sci. Total Environ.* 607, 413–432.
- El-Housni, H., Duchesne, S., Mailhot, A., 2019. Predicting individual hydraulic performance of sewer pipes in context of climate change. *J. Water Res. Plan. Man.* 145 (11), 04019051.
- Ene, S., Küçükoğlu, İ., Aksoy, A., ÖzTÜRK, N., 2016. A genetic algorithm for minimizing energy consumption in warehouses. *Energy* 114, 973–980.
- Fletcher, T.D., Shuster, W., Hunt, W.F., Ashley, R., Butler, D., Arthur, S., Trowsdale, S., Barraud, S., Semadeni-Dix, A., Bertrand-Krajewski, J.L., Mikkelsen, P.S., Rivard, G., Uhl, M., Dagenais, D., Vilklander, M., 2015. SUDS, LID, BMPs, WSUD and more - The evolution and application of terminology surrounding urban drainage. *Urban Water J* 12 (7), 525–542.
- Gao, X.J., Shi, Y., Han, Z.Y., Wang, M.L., Wu, J., Zhang, D.F., Xu, Y., Giorgi, F., 2017. Performance of RegCM4 over major river basins in China. *Adv. Atmos. Sci.* 34 (4), 441–455.
- Giorgi, F., Mearns, L., 1999. Introduction to special section: regional climate modeling revisited. *J. Geophys. Res.* 104, 6335–6352.
- Gong, Y., Yin, D., Li, J., Zhang, X., Wang, W., Fang, X., Shi, H., Wang, Q., 2019. Performance assessment of extensive green roof runoff flow and quality control capacity based on pilot experiments. *Sci. Total Environ.* 687, 505–515.
- Gong, Y.W., Liang, X.Y., Li, X.N., Li, J.Q., Fang, X., Song, R.N., 2016. Influence of rainfall characteristics on total suspended solids in urban runoff: a case study in Beijing, China. *Water-Sui* 8 (7).
- Haghghi, A., Bakhshipour, A.E., 2012. Optimization of sewer networks using an adaptive genetic algorithm. *Water Resour. Manage.* 26 (12), 3441–3456.
- Hallegatte, S., Green, C., Nicholls, R.J., Corfee-Morlot, J., 2013. Future flood losses in major coastal cities. *Nat. Clim. Change.* 3 (9), 802–806.
- Houle, J.J., Roseen, R.M., Ballesteros, T.P., Puls, T.A., Sherrard, J., 2013. Comparison of maintenance cost, labor demands, and system performance for LID and conventional stormwater management. *J. Environ. Eng.* 139 (7), 932–938.
- Hsu, C.-M., Chen, K.-Y., Chen, M.-C., 2005. Batching orders in warehouses by minimizing travel distance with genetic algorithms. *Comput. Ind.* 56 (2), 169–178.
- Hu, M.C., Zhang, X.Q., Li, Y., Yang, H., Tanaka, K., 2019. Flood mitigation performance of low impact development technologies under different storms for retrofitting an urbanized area. *J. Clean. Prod.* 222, 373–380.
- IPCC, 2014. Climate Change 2013 – The Physical Science Basis: Working Group I Contribution to the Fifth Assessment Report of the Intergovernmental Panel on Climate Change. Intergovernmental Panel On Climate, C. (ed.). Cambridge University Press, Cambridge, pp. 741–866.
- Islam, A., Hassini, S., El-Dakhakhni, W., 2021. A systematic bibliometric review of optimization and resilience within low impact development stormwater management practices. *J. Hydrol.* 599.
- Jehanzaib, M., Shah, S.A., Yoo, J., Kim, T.W., 2020. Investigating the impacts of climate change and human activities on hydrological drought using non-stationary approaches. *J. Hydrol.* 588, 125052.
- Jiang, C., Li, J., Li, H., Li, Y., Chen, L., 2017. Field performance of bioretention systems for runoff quantity regulation and pollutant removal. *Water Air and Soil Pollut.* 228 (12).

- Joo, J., Lee, J., Kim, J.H., Jun, H., Jo, D., 2014. Inter-event time definition setting procedure for urban drainage systems. *Water-Sui* 6 (1), 45–58.
- Kim, J., Lee, J., Song, Y., Han, H., Joo, J., 2018. Modeling the runoff reduction effect of low impact development installations in an industrial area, South Korea. *Water-Sui* 10 (8).
- Larsen, T.A., Hoffmann, S., Luthi, C., Truffer, B., Maurer, M., 2016. Emerging solutions to the water challenges of an urbanizing world. *Science* 352 (6288), 928–933.
- Lee, J.G., Selvakumar, A., Alvi, K., Riverson, J., Chen, J.X., Shoemaker, L., Lai, F.-h., 2012. A watershed-scale design optimization model for stormwater best management practices. *Environ. Modell. Softw.* 37, 6–18.
- Lim, H.S., Lu, X.X., 2016. Sustainable urban stormwater management in the tropics: an evaluation of Singapore's AWRS Waters Program. *J. Hydrol.* 538, 842–862.
- Liu, Y.Z., Ahiablame, L.M., Bralts, V.F., Engel, B.A., 2015. Enhancing a rainfall-runoff model to assess the impacts of BMPs and LID practices on storm runoff. *J. Environ. Manage.* 147, 12–23.
- Madarang, K., Kang, J.H., 2013. Accuracy of a stormwater monitoring program for urban landuses. *Water Environ. Res* 85 (9), 815–822.
- McFarland, A.R., Larsen, L., Yeshitela, K., Engida, A.N., Love, N.G., 2019. Guide for using green infrastructure in urban environments for stormwater management. *Environ. Sci.-Wat. Res.* 5 (4), 643–659.
- Mei, C., Liu, J.H., Wang, H., Yang, Z.Y., Ding, X.Y., Shao, W.W., 2018. Integrated assessments of green infrastructure for flood mitigation to support robust decision-making for sponge city construction in an urbanized watershed. *Sci. Total Environ.* 639, 1394–1407.
- Meinshausen, M., Smith, S.J., Calvin, K., Daniel, J.S., Kainuma, M.L.T., Lamarque, J.F., Matsumoto, K., Montzka, S.A., Raper, S.C.B., Riahi, K., Thomson, A., Velders, G.J.M., van Vuuren, D.P.P., 2011. The RCP greenhouse gas concentrations and their extensions from 1765 to 2300. *Clim. Change* 109 (1–2), 213–241.
- Ministry of Housing and Urban-Rural Development (MOHURD). 2016. Code for design of outdoor wastewater engineering. Beijing, People's Republic of China: MOHURD.
- Mohanty, M.P., Vittal, H., Yadav, V., Ghosh, S., Rao, G.S., Karmakar, S., 2020. A new bivariate risk classifier for flood management considering hazard and socio-economic dimensions. *J. Environ. Manage.* 255, 109733.
- Nazari-Sharabian, M., Taherioun, M., Karakouzian, M., 2019. Surface runoff and pollutant load response to urbanization, climate variability, and low impact developments - a case study. *Water Supply* 19 (8), 2410–2421.
- Nickel, D., Schoenfelder, W., Medearis, D., Dolowitz, D.P., Keeley, M., Shuster, W., 2014. German experience in managing stormwater with green infrastructure. *J. Environ. Plann. Man.* 57 (3), 403–423.
- Nika, C.E., Gusmaroli, L., Ghafourian, M., Atanasova, N., Buttiglieri, G., Katsou, E., 2020. Nature-based solutions as enablers of circularity in water systems: a review on assessment methodologies, tools and indicators. *WATER RES.* 183, 115988.
- Noor, M., Ismail, T., Shahid, S., Asaduzzaman, M., Dewan, A., 2022. Projection of rainfall intensity-duration-frequency curves at ungauged location under climate change scenarios. *Sustain. Cities. Soc.* 83, 103951.
- O'Neill, B.C., Tebaldi, C., van Vuuren, D.P., Eyring, V., Friedlingstein, P., Hurtt, G., Knutti, R., Kriegler, E., Lamarque, J.F., Lowe, J., Meehl, G.A., Moss, R., Riahi, K., Sanderson, B.M., 2016. The scenario model intercomparison project (ScenarioMIP) for CMIP6. *Geosci. Model. Dev.* 9 (9), 3461–3482.
- Pan, X.D., Zhang, L., Huang, C.L., 2020. Future climate projection in Northwest China with RegCM4.6. *Earth. Space Sci.* 7 (2).
- Qi, J.-D., He, B.-J., Wang, M., Zhu, J., Fu, W.-C., 2019. Do grey infrastructures always elevate urban temperature? No, utilizing grey infrastructures to mitigate urban heat island effects. *Sustain. Cities Soc.* 46, 101392.
- Rasheed, A., Egodawatta, P., Goonetilleke, A., McGree, J., 2019. A novel approach for delineation of homogeneous rainfall regions for water sensitive urban design-a case study in Southeast Queensland. *Water-Sui* 11 (3).
- Requena, A.I., Burn, D.H., Coulibaly, P., 2019. Estimates of gridded relative changes in 24-h extreme rainfall intensities based on pooled frequency analysis. *J. Hydrol.* 577, 123940.
- Rezaei, A.R., Ismail, Z., Niksokhan, M.H., Dayarian, M.A., Ramli, A.H., Yusoff, S., 2021. Optimal implementation of low impact development for urban stormwater quantity and quality control using multi-objective optimization. *Environ. Monit. Assess.* 193 (4).
- Rossman, L.A., 2010. Storm Water Management Model User's Manual, Version 5.0. National Risk Management Research Laboratory, Office of Research and Development, US Environmental Protection Agency.
- Rossman, L.A., Huber, W.C., 2016. Storm Water Management Model Reference Manual Volume I-Hydrology. US Environmental Protection Agency.
- Salim, I., Paule-Mercado, M.C., Sajjad, R.U., Memon, S.A., Lee, B.Y., Sukhbaatar, C., Lee, C.H., 2019. Trend analysis of rainfall characteristics and its impact on stormwater runoff quality from urban and agricultural catchment. *Membr. Water Treat.* 10 (1), 45–55.
- Shi, C., Jiang, Z.H., Zhu, L.H., Zhang, X.B., Yao, Y.Y., Li, L., 2020. Risks of temperature extremes over China under 1.5°C and 2°C global warming. *Adv. Clim. Chang. Res.* 11 (3), 172–184.
- Sohn, W., Kim, J.H., Li, M.H., Brown, R., 2019. The influence of climate on the effectiveness of low impact development: a systematic review. *J. Environ. Manage.* 236, 365–379.
- Versini, P.A., Kotelnikova, N., Poulhes, A., Tchiguirinskaia, I., Schertzer, D., Leurent, F., 2018. A distributed modelling approach to assess the use of Blue and Green Infrastructures to fulfil stormwater management requirements. *Landscape Urban Plann.* 173, 60–63.
- Wang, J., Cheng, Q.Y., Xue, S.G., Rajendran, M., Wu, C., Liao, J.X., 2018. Pollution characteristics of surface runoff under different restoration types in manganese tailing wasteland. *Environ. Sci. Pollut. Res.* 25 (10), 9998–10005.
- Wang, J., Liu, G.H., Wang, J.Y., Xu, X.L., Shao, Y.T., Zhang, Q., Liu, Y.C., Qi, L., Wang, H. C., 2021a. Current status, existent problems, and coping strategy of urban drainage pipeline network in China. *Environ. Sci. Pollut. Res.* 28 (32), 43035–43049.
- Wang, M., Zhang, Y., Bakhshiour, A.E., Liu, M., Rao, Q., Lu, Z., 2022. Designing coupled LID-GREI urban drainage systems: Resilience assessment and decision-making framework. *Science of The Total Environment* 834, 155267.
- Wang, M., Zhang, D.Q., Su, J., Trzcienski, A.P., Dong, J.W., Tan, S.K., 2017a. Future scenarios modeling of urban stormwater management response to impacts of climate change and urbanization. *Clean-Soil Air Water* 45 (10).
- Wang, M., Zhang, D.Q., Wang, Z.L., Zhou, S.Q., Tan, S.K., 2021b. Long-term performance of bioretention systems in storm runoff management under climate change and life-cycle condition. *Sustain. Cities. Soc.* 65, 102598.
- Wang, M., Zhang, Y., Zhang, D.Q., Zheng, Y.S., Li, S., Tan, S.K., 2021c. Life-cycle cost analysis and resilience consideration for coupled grey infrastructure and low-impact development practices. *Sustain. Cities. Soc.* 75, 103358.
- Wang, M., Zhang, Y., Zhang, D.Q., Zheng, Y.S., Zhou, S.Q., Tan, S.K., 2021d. A Bayesian decision model for optimum investment and design of low-impact development in urban stormwater infrastructure and management. *Front. Env. Sci.-Switz.* 9, 713831.
- Wang, M.M., Sweetapple, C., Fu, G.T., Farmani, R., Butler, D., 2017b. A framework to support decision making in the selection of sustainable drainage system design alternatives. *J. Environ. Manag.* 201, 145–152.
- Wang, Z.L., Zhou, S.Q., Wang, M., Zhang, D.Q., 2020. Cost-benefit analysis of low-impact development at hectare scale for urban stormwater source control in response to anticipated climatic change. *J. Environ. Manage.* 264, 110483.
- Willems, P., Arnbjerg-Nielsen, K., Olsson, J., Nguyen, V.T.V., 2012. Climate change impact assessment on urban rainfall extremes and urban drainage: methods and shortcomings. *Atmos. Res.* 103, 106–118.
- Wu, C.H., Huang, G.R., 2016. Projection of climate extremes in the Zhujiang River basin using a regional climate model. *Int. J. Climatol.* 36 (3), 1184–1196.
- Xing, W., Li, P., Cao, S.-b., Gan, L.-l., Liu, F.-l., Zuo, J.-e., 2016. Layout effects and optimization of runoff storage and filtration facilities based on SWMM simulation in a demonstration area. *Water Sci. Eng.* 9 (2), 115–124.
- Xu, C.Q., Hong, J.L., Jia, H.F., Liang, S.D., Xu, T., 2017. Life cycle environmental and economic assessment of a LID-BMP treatment train system: a case study in China. *J. Clean. Prod.* 149, 227–237.
- Xu, C.Q., Tang, T., Jia, H.F., Xu, M., Xu, T., Liu, Z.J., Long, Y., Zhang, R.R., 2019. Benefits of coupled green and grey infrastructure systems: evidence based on analytic hierarchy process and life cycle costing. *Resour. Conserv. Recycl.* 151, 104478.
- Yang, W.Y., Zhang, J., 2021. Assessing the performance of gray and green strategies for sustainable urban drainage system development: a multi-criteria decision-making analysis. *J. Clean. Prod.* 293, 126191.
- Ying, J., Zhang, X.J., Zhang, Y.Q., Bilan, S., 2021. Green infrastructure: systematic literature review. *Econ. Res-Ekon. Istraz.*
- Yu, Y., Chen, L., Xiao, Y.C., Chang, C.C., Zhi, X.S., Shen, Z.Y., 2022. New framework for assessing urban stormwater management measures in the context of climate change. *Sci. Total Environ.* 813, 151901.
- Zeng, J.J., Lin, G.S., Huang, G.R., 2021. Evaluation of the cost-effectiveness of Green Infrastructure in climate change scenarios using TOPSIS. *Urban For. Urban Green.* 64, 127287.
- Zhang, H., Yang, Z.F., Cai, Y.P., Qiu, J., Huang, B.S., 2021. Impacts of climate change on urban drainage systems by future short-duration design rainstorms. *Water-Sui* 13 (19), 2718.
- Zhou, S., Liu, Z., Wang, M., Gan, W., Zhao, Z., Wu, Z., 2022. Impacts of building configurations on urban stormwater management at a block scale using XGBoost. *Sustain. Cities Soc.* 87, 104235.